




Synthesis, crystal structures, Hirshfeld surface analysis and physico-chemical characterization of two new Zn^{II} and Cd^{II} halidometallates

Ali Rayes¹, Manel Moncer¹, Irene Ara², Necmi Dege³, and Brahim Ayed^{4,5,*} 

¹Laboratoire de Recherche, Catalyse et Matériaux pour l'Environnement et les Procédés, LRCMEP, (LR19ES08), Faculté des Sciences de Gabès, Campus Universitaire, 6072 Gabès, Tunisia

²Departamento de Química Inorgánica, Instituto de Síntesis Química y Catálisis Homogénea (ISQCH) CSIC-Universidad de Zaragoza, C/Pedro Cerbuna 12, 50009 Zaragoza, Spain

³Faculty of Arts and Sciences, Department of Physics, Ondokuz Mayıs University, 55139 Samsun, Turkey

⁴Unité de Recherche Analyses et Procédés Appliqués à l'Environnement, Institut Supérieur des Sciences Appliquées et de Technologie de Mahdia, Université de Monastir, Monastir, Tunisia

⁵Laboratoire de recherche, Physico-chimie des Matériaux, Faculté des Sciences de Monastir, Université de Monastir, Monastir, Tunisia

Received: 11 January 2021

Accepted: 10 March 2021

Published online:
29 March 2021

© The Author(s) 2021

ABSTRACT

Two new organic–inorganic hybrid materials, based on 1,3-CycloHexaneBis(Methyl Amine), abbreviated CHBMA, namely (H₂CHBMA)ZnCl₄·2H₂O (CP1) and (H₂CHBMA)CdI₄·2H₂O (CP2), have been synthesized under mild conditions in acidic media and characterized by single-crystal X-ray diffraction, spectroscopic techniques (¹³C NMR, FTIR, RAMAN) and thermal analysis. The crystal structures of the two compounds were solved by single-crystal X-ray diffraction methods. Both compounds show a 3-dimensional supramolecular structure directed by various interactions between tetrahalidometallate anions (ZnCl₄²⁻, CdI₄²⁻), water molecule and organic cations (H₂CHBMA)²⁺. For both compounds, the cyclohexane ring of the template cation is in a chair conformation with the methylammonium substituent in the equatorial positions and the two terminal ammonium groups in a cis conformation but with two different orientations (upward for CP1 and downward for CP2) which influences the supramolecular architecture of the two structures. Hirshfeld surface analysis and the associated two-dimensional finger print plots were used to explore and quantify the intermolecular interactions in the crystals.

Address correspondence to E-mail: ayedbrahim@yahoo.com

1 Introduction

In recent years, hybrid compounds represent a novel class of materials that could combine both organic and inorganic components into a single material in the solid state [1, 2]. Inside the structures of these materials, the organic and inorganic components are connected through covalent, ionic or hydrogen bonds. This symbiosis between organic and inorganic domains of chemistry considered for a long time as antagonists and can also be conducted to totally new properties, which opens up a new and an ample area of research in chemistry. In particular, metal-halides may be assembled with organic amines to generate two different categories of hybrid materials based on the bonding chemical nature between organic molecule and inorganic units. This means that the structure of the final product and its properties are dependent on many factors, such as the selection of organic amine molecule, the suitable metal halide and the synthesis conditions (pH value of the reaction medium, anions, temperature, solvent type, etc.) [3].

When the organic amine and the metal ion or metal halide are connected together via strong chemical bonds (covalent, ionic-covalent or coordination bonds), the resulting product being part of organically coordinated metal halide family. The design and construction of these complexes have been attracted significant attention due to their fascinating structures and their promising applications in diverse fields such as catalysis [4–6], fluorescence and sensing [7], medicinal chemistry as pharmaceutical compounds [8, 9]. In this case, the choice of organic amine ligand is especially significant in obtaining desirable materials, because the architecture of coordination complexes can be considerably impacted by the shape, symmetry, flexibility and the number of amine groups available for coordination. It is well known that structural geometry changes have an important impact on the properties of the final complexes [10].

When the components are associated as perhalidometallate anions and organic cations, the resulting products belong to the organically templated perhalidometallate family. In that event, the cohesion of the whole structure is ensured only by weak bonds, namely hydrogen bonding, ionic bonds and Van der Waals interactions. The class of these hybrid compounds is very wide and very often conserves the properties of the individual parts, i.e., the

organic component offer structural diversity (great flexibility in the choice of molecules, length, polarizability, degree of saturation...) and also remarkable luminescent properties and potential conductivity, while the inorganic component potentially contributes to thermal stability, mechanical resistance, interesting magnetic or ferroelectric transitions and electric properties (conductor, semiconductor, insulator...) [11, 12]. Most of these ionic organic–inorganic hybrid metal halides experience multiple structural phase transitions frequently related to the reorientation dynamics of the organic ammonium groups [13–16] and some even show interesting physical properties, such as pyroelectricity, ferroelectricity, ferroelasticity and low dimensional magnetism [13, 17, 18]. Moreover, these materials were applied as catalysts in catalytic reactions such as acetylation [19], Henry reaction [20] at room temperature under mild conditions in the presence of methanol, as solvent. As a contribution to the investigation of the above materials, we report the synthesis, crystal structure study, Hirshfeld surface analysis, spectroscopic measurement and thermal analysis of two novel organically templated perhalidometallates, namely $(\text{H}_2\text{CHBMA})\text{ZnCl}_4 \cdot 2\text{H}_2\text{O}$ (CP1) and $(\text{H}_2\text{CHBMA})\text{CdI}_4 \cdot 2\text{H}_2\text{O}$ (CP2) where CHBMA is 1,3-CycloHexaneBis(MethylAmine).

2 Experimental section

2.1 Materials and methods

All the used chemicals [Zinc(II) chloride (ZnCl_2), Cadmium(II) iodide (CdI_2), Hydrochloric acid (HCl; 37%), Sulfuric acid (H_2SO_4 ; 98%) and 1,3-CycloHexaneBis (MethylAmine), abbreviated CHBMA, were obtained from commercial sources and used without further purification. CHBMA was purchased from Aldrich as a mixture of cis and trans isomers.

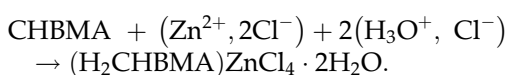
Infrared spectrum was recorded at a room temperature on a Nicolet 470 FTIR spectrophotometer in the $4000\text{--}400\text{ cm}^{-1}$ region. Thin transparent pellet was made by compacting an intimate mixture obtained by shaking 2 mg of the sample in 100 mg of KBr. Thermogravimetric and differential thermal analyses (TGA-TDA) were carried out on a Setaram TG-DTA 92-16.18 thermal analyzer. Sample was placed in an open platinum crucible and heated, under air, from room temperature to $600\text{ }^\circ\text{C}$ with

10 °C/min heating rate; an empty crucible was used as reference.

2.2 Synthesis

2.2.1 Synthesis of $(\text{H}_2\text{CHBMA})\text{ZnCl}_4 \cdot 2\text{H}_2\text{O}$, (CP1)

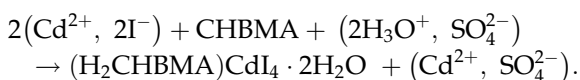
Crystals of $(\text{H}_2\text{CHBMA})\text{ZnCl}_4 \cdot 2\text{H}_2\text{O}$ (CP1) were obtained by slow evaporation, at room temperature. 1,3-CycloHexyl(Methyl Amine) (CHBMA) was dissolved with ZnCl_2 in 15 ml of distilled water and hydrochloric acid HCl with the metal/amine/acid molar ratio of 1:1:2. The reaction can be schematically written as



The reaction mixture was stirred for about a period of 20 min until the complete dissolution. After slow evaporation of the solution at room temperature during a period of 7 days, air stable colorless crystals of CP1 suitable for X-ray diffraction were selected (yield 55%).

2.2.2 Synthesis of $(\text{H}_2\text{CHBMA})\text{CdI}_4 \cdot 2\text{H}_2\text{O}$, (CP2)

The new compound $(\text{H}_2\text{CHBMA})\text{CdI}_4 \cdot 2\text{H}_2\text{O}$ (CP2) was synthesized by slow evaporation, at room temperature. 1,3-cyclohexyl(methylamine) (CBM) was dissolved with CdI_2 in about 20 ml of distilled water and sulfuric acid H_2SO_4 with the metal/amine/acid molar ratio of 2:1:1. The reaction can be schematically written as



After stirring over a period of about 30 min, the final mixture was preserved at room temperature. After a few days, colorless crystals appeared (yield 49%), from which crystals suitable for X-ray analysis were chosen. In addition, they are also stable in normal conditions of temperature and humidity.

2.3 Crystal structure determination and refinement

The crystal structures of compounds (CP1) and (CP2) were determined by single-crystal X-ray diffraction. The crystal parameters and experimental details of the data collection are summarized in Table 1. All H

atoms were located in difference Fourier maps. C- and N-bound H atoms were included in calculated positions and refined with isotropic displacement parameters riding on those of the parent atoms. The H atoms of the water molecules of CP1 were refined freely, while those of CP2 were placed in their expected calculated positions and refined as riding, with OW-H = 0.85 Å and with $U_{\text{iso}} = 1.5 U_{\text{eq}}$ (OW).

2.4 Hirshfeld surface calculation

The Hirshfeld surfaces and their corresponding two-dimensional fingerprint plots were calculated using the CrystalExplorer [21] software package, which accepts a structure input file in the CIF format. Graphical plots of the Hirshfeld surfaces are mapped with the normalized contact distance (d_{norm}), and these points out the regions of particular importance to intermolecular interactions. To visualize the intermolecular interactions on the Hirshfeld surface mapped over d_{norm} , a color scale of red, white or blue is used when the intermolecular contacts are shorter, equal or longer than the van der Waals separation, respectively. The two-dimensional fingerprint plot supplies breakdown of Hirshfeld surfaces into relative contribution of different intermolecular interactions existing in the crystal structures.

3 Results and discussion

3.1 Structure description

3.1.1 $(\text{CBMH}_2)\text{ZnCl}_4 \cdot 2\text{H}_2\text{O}$, (CP1)

The single-crystal X-ray diffraction investigation has exhibited that the new organic–inorganic hybrid compound CP1 crystallizes in the monoclinic system with space group $\text{P}2_1/\text{c}$. The asymmetric unit is made up of one $(\text{H}_2\text{CHBMA})^{2+}$ organic cation, an isolate $[\text{ZnCl}_4]^{2-}$ anion and two crystallographically independent uncoordinated molecules water as shown in Fig. 1a. The cohesion between these entities is ensured by a complex hydrogen-bonding system and by Columbic interactions. The distribution of the different species is shown in Fig. 2c.

The central divalent Zn is surrounded by four chlorine atoms in a slightly distorted tetrahedral geometry. The bond length of the Zn–Cl lies in the range 2.2590 (5) – 2.2989 (5) Å ($\text{Zn–Cl}_{\text{av}} = 2.274$ Å)

Table 1 Experimental details

| | CP1 | CP2 |
|---|--|--|
| Crystal data | | |
| Chemical formula | (CBMH ₂)ZnCl ₄ ·2H ₂ O | (CBMH ₂)CdI ₄ ·2H ₂ O |
| Formula weight (g mol ⁻¹) | 387.46 | 800.29 |
| Crystal system, space group | Monoclinic, P2 ₁ /c | Monoclinic, P2 ₁ /m |
| Temperature (K) | 293 | 293 |
| <i>a</i> , <i>b</i> , <i>c</i> (Å) | 6.791, 19.122, 13.139 | 7.2260 (4), 13.4994 (10), 10.4976 (6) |
| (°) | 99.77 | 95.774 (4) |
| <i>V</i> (Å ³) | 1681.5 | 1018.81 (11) |
| <i>Z</i> | 4 | 2 |
| Radiation type | Mo K | Mo K |
| (mm ⁻¹) | 2.089 | 7.128 |
| Crystal size (mm) | 0.32 0.18 0.10 | 0.14 0.11 0.08 |
| Data collection | | |
| Diffractometer | Bruker SMART CCD | Bruker APPEXII |
| Absorption correction | Multi-scan (SADABS; Bruker, 2008) | |
| No. of measured, independent and observed [<i>I</i> 2 (<i>I</i>)] reflections | 18,449, 3130, 2816 | 6486, 2080, 1826 |
| <i>R</i> _{int} (<i>sin</i>)/ _{max} (Å ⁻¹) | 0.030 | 0.046 |
| Refinement | | |
| <i>R</i> [<i>F</i> ² > 2(<i>F</i> ²)], <i>wR</i> (<i>F</i> ²), <i>S</i> | 0.026, 0.068, 1.07 | 0.0367, 0.0841, 1.121 |
| No. of reflections | 3130 | 2080 |
| No. of parameters | 172 | 89 |
| No. of restraints | 0 | 0 |
| H-atom treatment | H atoms treated by a mixture of independent and constrained refinement | H atoms treated by a mixture of independent and constrained refinement |
| <i>max</i> , <i>min</i> (e Å ⁻³) | 0.44, - 0.17 | 0.761, - 0.943 |

and the bond angles Cl–Zn–Cl vary from 104.23 (2) to 114.49 (2)° (Cl–Zn–Cl_{av} = 109.44°), which are in agreement with those observed in analogous compounds [22–25]. These geometric parameters in ZnCl₄²⁻ are related to the number of hydrogen bonds accepted by the Cl atoms. To quantify the distortion of the [ZnCl₄]²⁻ anion from the ideal tetrahedral conformation, τ_4 is a structural parameter introduced by Yang et al. [26] which can be used to gauge mainly the geometries of four-coordinate metal complexes. This parameter is defined as $\tau_4 = \frac{360-(\alpha)}{360-2}$, where α and β are the two largest valence angles around the central atom and $\theta = 109.5^\circ$ is the ideal tetrahedral angle. τ_4 can vary from 0 to 1, passing from an absolute square planar to an ideal tetrahedral conformation. The τ_4 value of the present structure is 0.952 which proves a little distortion of the Zn atom from a regular tetrahedron. BVS calculations using the Brown

and Altermatt method [27] revealed that the zinc atom have valence sums equal with a value of 2.045, close to the ideal value of 2 for Zn^{II}.

In the crystal structure, the four chlorine atoms of the [ZnCl₄]²⁻ anion are acting as acceptors of hydrogen bonds. Each ZnCl₄²⁻ anion bridges the water molecules (O1W, O2W) by means of O–HCl hydrogen bonds, forming an infinite two-dimensional supramolecular (ZnCl₄-OW)_n sheets extending parallel to (001) plane (Table 2, Fig. 2b). Within the anionic supramolecular layers, rings with graph-motif [28] are observed, lying at $x = \frac{1}{2}$. (Fig. 2c)

The (H₂CHBMA)²⁺ cations are confined between these anionic layers to maximize the electrostatic interactions and are connected to CdI₄²⁻ anion and H₂O molecule via N–H1C...OW, NH1A...I1, N–H1B...I3 and C5–H5A...I3 hydrogen bonds, thus forming a three-dimensional supramolecular

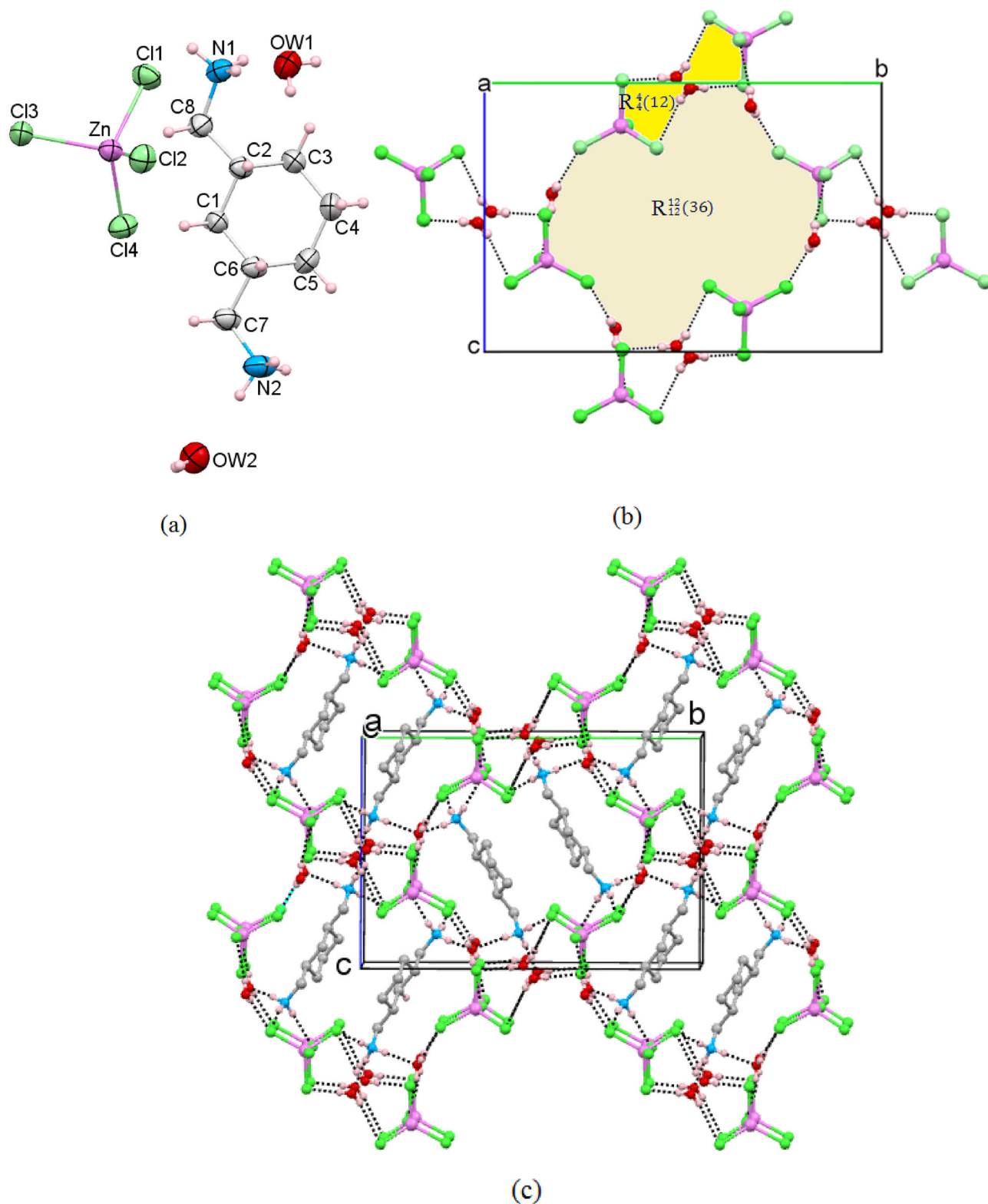


Fig. 1 **a** Displacement ellipsoid plot of the asymmetric unit of CP1, with ellipsoids drawn at the 50% probability level. **b** A layer of $(\text{ZnCl}_4\text{-OW})$ anions, parallel to the bc plane, formed by hydrogen bonds displaying $R_{12}^{12}(36)$ and $R_4^1(12)$ graph-set ring

motifs. **c** Packing diagram of the title compound viewed approximately along the a axis, showing the three-dimensional hydrogen bonding network (dashed lines)

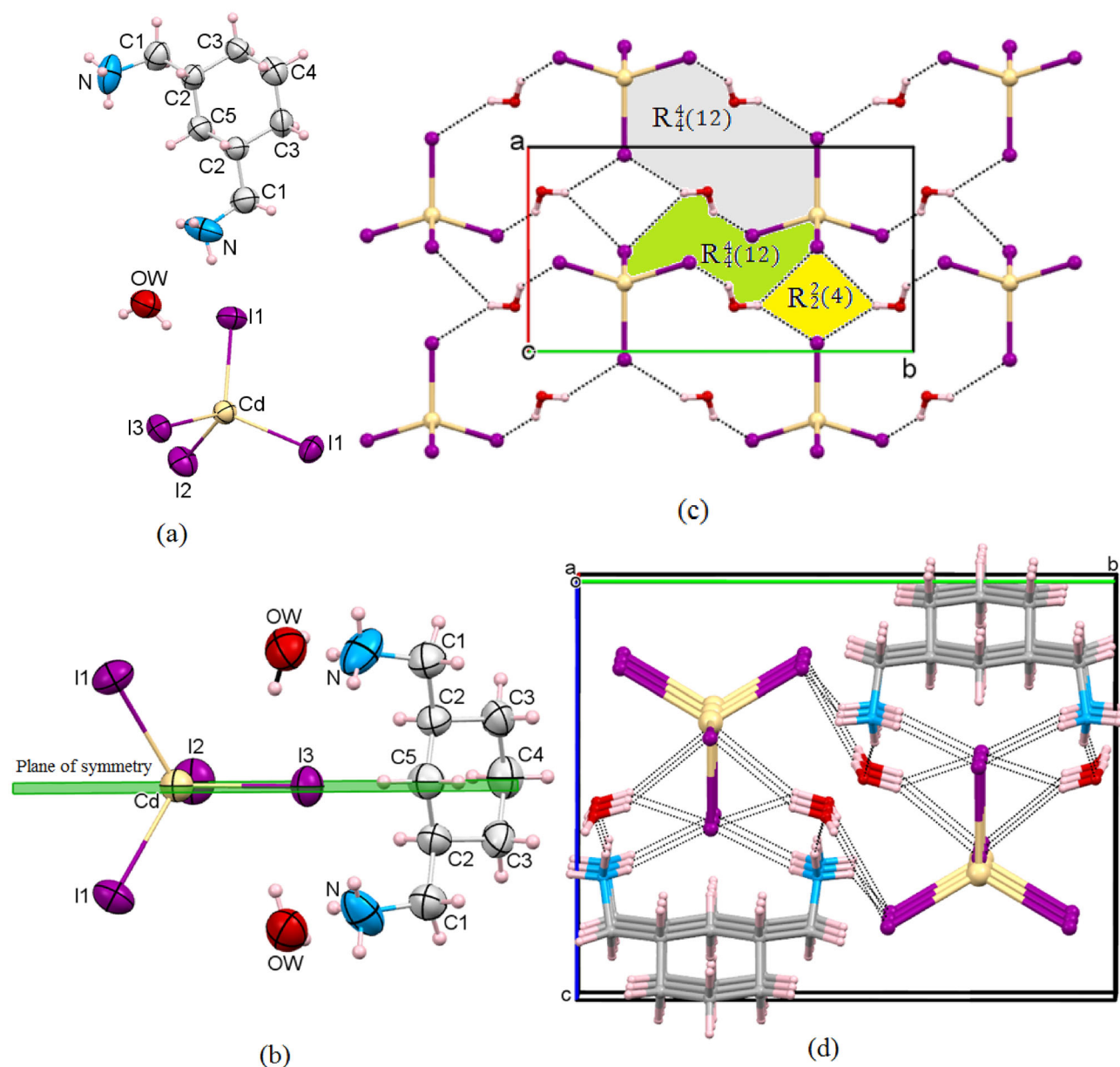


Fig. 2 **a** Displacement ellipsoid plot of the formula unit of CP2, with ellipsoids drawn at the 50% probability level. **b** Specific crystallographic location of CP2. **c** A layer of $(\text{CdL}_4\text{-OW})$ anions, parallel to the ab plane, formed by hydrogen bonds displaying

structure. Hence, each $(\text{CBMH}_2)^{2+}$ cation engages its hydrogen atoms bonded to N1 and N2 atoms in hydrogen bonds and participates in the structure stability via intermolecular H-bonds established between the organic and inorganic layers. The hydrogen-bond details are given in Table 2 and are shown in Fig. 1c. The hydrogen-bond interactions link the three components into a supramolecular 3D network.

$R_2^2(4)$ and $R_4^1(12)$ graph-set ring motifs. **d** Packing diagram of the title compound viewed approximately along the a axis, showing the two-dimensional hydrogen-bonding network (dashed lines)

In CP1, the C6-ring of the template cation adopts a typical chair conformation, four carbon atoms are coplanar, and the other two are puckered out of this plane, with normal distances C–C, C–N and angles C–C–C, C–C–N (Table 3). Interestingly, although CBM was employed as a mixture of cis and trans isomers. Similar phenomenon was observed in the preparation of TJPU3, in which solely cis CBM is used as template [29].

Table 2 Hydrogen-bond geometry (Å, °) in (CBMH₂)ZnCl₄·2H₂O

| D-HA | D-H | HA | DX | D-HX |
|---------------------------|----------|----------|-----------|---------|
| N1-H1CO1 | 0.89 | 2.03 | 2.899 (3) | 165 |
| N1-HIDCl4 ⁱ | 0.89 | 2.38 | 3.258 (2) | 170 |
| N1-H1ECI3 ⁱⁱ | 0.89 | 2.34 | 3.210 (7) | 166 |
| N2-H2ACI2 ⁱⁱⁱ | 0.89 | 2.76 | 3.634 (2) | 166 |
| N2-H2BO2 | 0.89 | 1.95 | 2.838 (3) | 176 |
| N2-H2CO1 ^{iv} | 0.89 | 2.07 | 2.950 (3) | 170 |
| C1-H1BCI4 | 0.97 | 2.83 | 3.720 (2) | 154 |
| O1-H1O1-Cl4 ⁱⁱ | 0.77 (3) | 2.62(3) | 3.331(2) | 153 (3) |
| O1-H2O1-Cl3 ^v | 0.78 (4) | 2.52 (4) | 3.292 (2) | 168 (4) |
| O2-H1O2-Cl1 ^{vi} | 0.85 (4) | 2.52 (4) | 3.369 (2) | 174 (3) |
| O2-H2O2-Cl2 ^{iv} | 0.76 (4) | 2.63 (4) | 3.348 (2) | 158 (4) |

Symmetry codes: (i) $x, -y + 1/2, z - 1/2$; (ii) $x - 1, -y + 1/2, z - 1/2$; (iii) $-x, y + 1/2, -z + 3/2$; (iv) $x, -y + 1/2, z + 1/2$; (v) $x - 1, y, z$; (vi) $-x + 1, y + 1/2, -z + 3/2$

3.1.2 (H₂CHBMA)CdI₄·2H₂O, (CP2)

CP2 crystallizes in the monoclinic centrosymmetric space group P2₁/m; the formula unit contains one (CBMH₂)²⁺ cation, one CdI₄²⁻ anion and two molecules water of crystallization (Fig. 2a). As shown in Fig. 2b, the central Cd^{II} atom, together with I2 and I3 atoms of the CdI₄²⁻ anion, and carbon atoms C4 and

C5 of the cyclohexane ring lie in a specific crystallographic location, namely on mirror plane *m*. The remaining atoms of the cation, anion and water molecules, lying outside the plane, are necessarily mirror images of each other. Crystal structure study proves that in CP2, the Cd^{II} ion is in a slightly distorted tetrahedral geometry, with a four-coordinate index, τ_4 [26], of 0.97. Selected bond lengths and angles are listed in Table 4 and are in agreement with the values reported for analogous compounds [30–32]. The bond angles implying the Cd^{II} atom range between 100.130 (3) and 111.585 (1) Å. The short value, significantly smaller than all the other bond angles, is observed for the I2–Cd–I3 angle. This distortion can be explained by the fact that the iodine atoms are involved in a complex system of hydrogen bonds O(N)–H···I responsible for the phenomenon.

In the material, the discrete CdI₄²⁻ anions alternately bridge the water molecules (OW) via O–H···I hydrogen bonds, building an infinite two-dimensional supramolecular {CdI₄–OW}_n undulated layers extending parallel to (001) plane (Fig. 2c). Within the anionic supramolecular layer, rings with a graphmotif [28] are observed, lying at $x = 1/2$ (Fig. 2c). The (H₂CHBMA)²⁺ cations are confined between these anionic layers to maximize the electrostatic interactions and are connected to CdI₄²⁻ anion and H₂O

Table 3 Selected bond distances (Å) and angles (°) in (CBMH₂)ZnCl₄·2H₂O

| Angles (°) | | Distances (Å) | |
|--|-------------|---------------|------------|
| Tetrahedron [ZnCl ₄] ²⁻ | | | |
| Cl2–Zn–Cl4 | 110.83 (2) | Zn–Cl1 | 2.2768 (6) |
| Cl2–Zn–Cl1 | 108.57 (2) | Zn–Cl2 | 2.2590 (5) |
| Cl4–Zn–Cl1 | 114.49 (2) | Zn–Cl3 | 2.2989 (5) |
| Cl2–Zn–Cl3 | 111.26 (2) | Zn–Cl4 | 2.2640 (6) |
| Cl4–Zn–Cl3 | 107.30 (2) | | |
| Cl1–Zn–Cl3 | 104.23(2) | | |
| Organic molecule | | | |
| C5–C4–C3 | 112.45 (18) | C8–N1 | 1.491 (3) |
| C2–C1–C6 | 111.94 (18) | C7–N2 | 1.491 (3) |
| C4–C3–C2 | 112.15 (16) | C1–C2 | 1.525 (3) |
| C8–C2–C3 | 113.90 (17) | C1–C6 | 1.527 (3) |
| C8–C2–C1 | 108.41 (16) | C2–C8 | 1.518 (3) |
| C3–C2–C1 | 110.45 (16) | C2–C3 | 1.519 (3) |
| C2–C3–C4 | 111.45 (18) | C3–C4 | 1.522 (3) |
| C7–C6–C5 | 113.87 (18) | C4–C5 | 1.520 (3) |
| C7–C6–C1 | 108.69 (16) | C5–C6 | 1.518 (3) |
| C5–C6–C1 | 110.25 (16) | C6–C7 | 1.512 (3) |
| N2–C7–C6 | 112.68 (17) | | |
| N1–C8–C2 | 112.76 (17) | | |

Table 4 Selected bond distances (Å) and angles (°) in (CBMH₂)CdI₄·2H₂O

| Angles (°) | | Distances (Å) | |
|---|--------------|---------------|------------|
| Tetrahedron [CdI ₄] ²⁻ | | | |
| I1–Cd–I1 | 110.90 (3) | Cd–I1 | 2.7593 (6) |
| I1–Cd–I2 | 111.113 (18) | Cd–I2 | 2.7735 (9) |
| I1–Cd–I3 | 111.585 (18) | Cd–I3 | 2.8162 (9) |
| I2–Cd–I3 | 100.13 (3) | | |
| Organic molecule | | | |
| C3–C2–C5 | 111.2 (6) | C2–C3 | 1.496 (9) |
| C3–C2–C1 | 109.3 (6) | C2–C5 | 1.503 (8) |
| C5–C2–C1 | 111.7 (6) | C2–C1 | 1.520 (9) |
| C2–C5–C2 | 110.9 (7) | N1–C1 | 1.470 (10) |
| C2–C3–C4 | 110.0 (6) | C3–C4 | 1.509 (9) |
| C3–C4–C3 | 111.4 (8) | | |
| N1–C1–C2 | 112.7 (6) | | |

molecule via N–H1C...OW, N–H1A...I1, N–H1B...I3 and C5–H5A...I3 hydrogen bonds, thus forming a three-dimensional supramolecular structure.

It is worth to note that the existence of the uncoordinated water molecule consolidates the H-bonding network. It can participate as H-bond donor with the iodide ligands of the isolated tetrahedral CdI₄²⁻ units (OW–H2...I1, OW–H2...I2, OW–H1...I3) and as H-bond acceptor with the positively charged ammonium groups of (CBMH₂)²⁺ cations ((N–H1C...OW)). The hydrogen-bond details are given in Table 5 and are shown in Fig. 2d. The hydrogen-bond interactions link the CdI₄²⁻ anion, (CBMH₂)²⁺ cations and H₂O molecule, to create a two-dimensional (2D) hydrogen-bond network.

Other interesting noticing is the template CHBMA molecule. As in the case of compound CP1, the cyclohexane ring of the organic cation in CP2 adopts also a chair conformation which is the most stable.

Table 5 Hydrogen-bond geometry (Å, °) in (CBMH₂)CdI₄·2H₂O

| D–HA | D–H | HA | DX | D–HX |
|----------|------|-------|-----------|--------|
| N1–H1A11 | 0.89 | 3.06 | 3.677 (7) | 127.94 |
| N1–H1B13 | 0.89 | 3.07 | 3.957 (8) | 172.6 |
| N1–H1COW | 0.89 | 2.01 | 2.871 (9) | 162.3 |
| OW–H1A11 | 0.85 | 2.935 | 3.663 (6) | 140.64 |
| OW–H1B12 | 0.85 | 3.084 | 3.793 (6) | 142.47 |
| OW–H1B13 | 0.85 | 3.067 | 3.647 (7) | 127.53 |

Furthermore, although CBM molecule was used as a mixture of cis and trans isomers, the two methylamine groups exist in the cis conformation in both CP1 and CP2. For the same cis conformation, the two terminal ammonium groups in organic moiety are pointing upward for CP1 and downward for CP2. This difference has an impact on the topological nature of the anionic layers and this reflecting in a different anchoring of the organic cations on the anionic layers, building a three-dimensional hydrogen-bonded network in the case of CP1 and two-dimensional hydrogen-bonded network in the case of CP2.

Interestingly, the syntheses of CP1 and CP2 show selectivity for cis CBM isomers. The trans conformation has been also observed with the same organic cation (CBMH₂)²⁺ in other compounds [29, 33]. This may be a possible technique for separation and recognition of cis and trans isomers of CBM.

3.2 Hirshfeld surface analysis

Hirshfeld surface analysis has been carried out in order to decrypt and quantify the intermolecular interactions involved in the crystal packing of compounds CP1–CP2. Figure 3 displays Hirshfeld surfaces mapped over the d_{norm} (normalized contact distance) property in two orientations and the associated full 2-dimensional fingerprint plots. The surfaces are represented as transparent to permit visualization of all atoms of the asymmetric unit for the title compounds. To visualize the intermolecular interactions in the d_{norm} map, a color scale is used. The red implies contacts with distances shorter than the sum of van der Waals (vdW) radii, while the blue and white regions indicate contacts with distances longer than and equal to the sum of Van der Waals radii, respectively [34]. For both compounds, the different intermolecular contacts are quantified with the breaking down of the full fingerprint region and their relative contributions, in percentage terms, to the overall crystal packing are exhibited as histograms in Fig. 3.

In compound CP1, the large red spots labeled 1' in Fig. 3 represent H...Cl/Cl...H contacts, which are relevant in the d_{norm} maps. These contacts are attributed to N–H...Cl and O–H...Cl hydrogen bonds, which can be seen in the finger print as a pair of symmetrical spikes at ($d_e + d_i$; 2.30 Å) in agreement with the expected higher strength for N1–H1E...Cl3

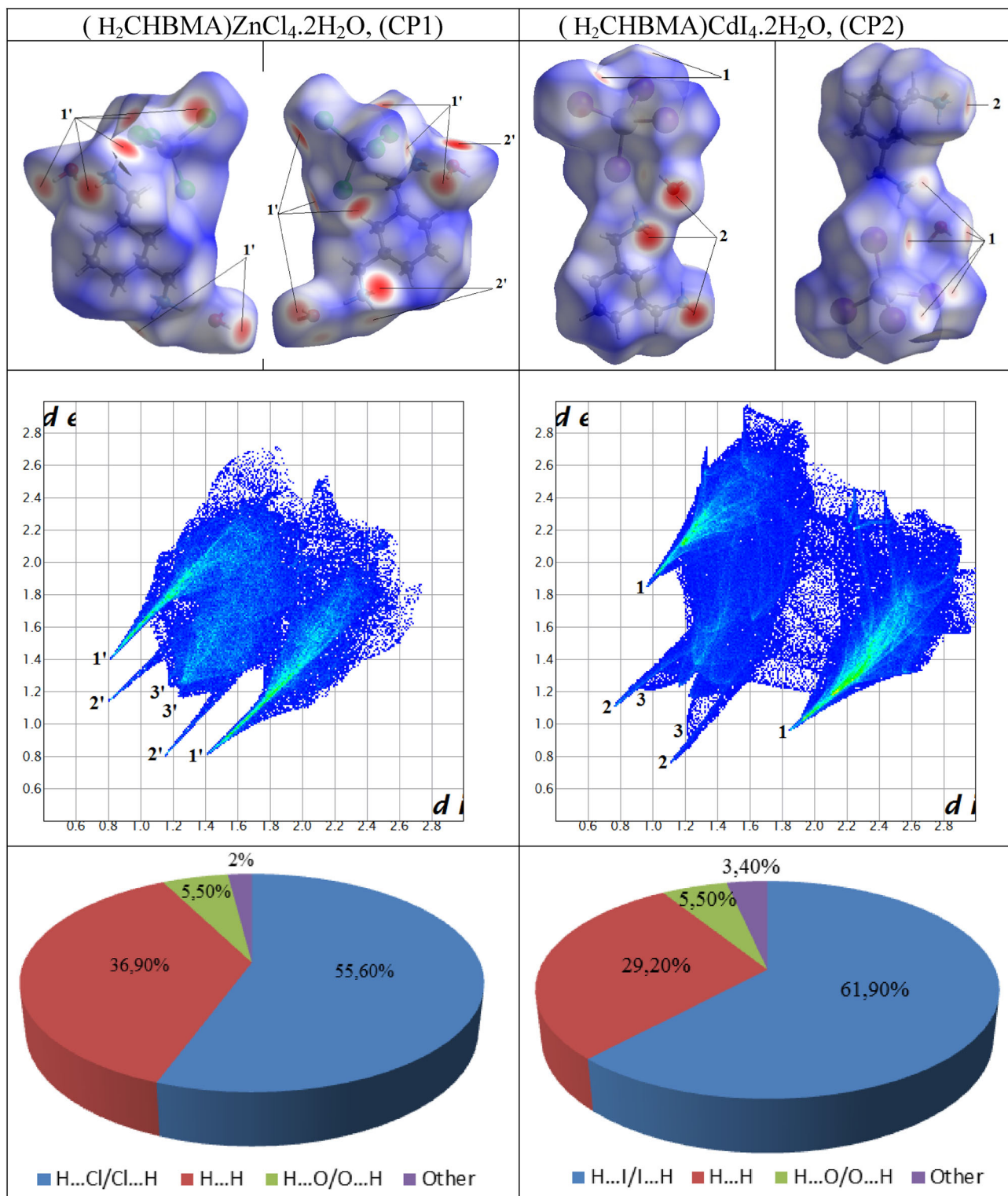


Fig. 3 Views of the Hirshfeld surfaces mapped with d_{norm} in two orientations (front view and back view), the full 2D fingerprint plots and the relative contributions to the Hirshfeld surface area of the various close intermolecular contacts in compounds CP1 and CP2

hydrogen bond (Table 2). The H...Cl/Cl...H contacts are dominant for the complex CP1 with higher

contributions of 55.6% of the overall packing (Fig. 3). The large deep-red spots labeled 2' in the d_{norm} show

also strong H···O/O···H contacts attributed to N–H···O hydrogen bonds, which are viewed as a pair of symmetrical spikes with minimum ($d_e + d_i$ 1.94 Å) in agreement with the anticipated higher strength for N2–H2B···O2W. The H···O/O···H represent 5.5% of the total Hirshfeld surface area. The H···H interactions labeled 3' in Fig. 3, contributing 36.90% to the overall crystal packing. The two symmetrical broad peaks in the middle region of fingerprint with minimum contact ($d_e + d_i = 2.4$ Å) are due to a short interatomic H···H contact.

In compound CP2, the H···I/I···H contacts labeled 1 in Fig. 3 have the highest contribution (61.90%) to the overall Hirshfeld surface area. These contacts which appear as tiny red spots in the d_{norm} surface are attributed to N–H···I and O–H···I hydrogen bonds. The next most contribution to the overall crystal packing arises from the H···H and H···O/O···H interactions, respectively. In fact, the H···H contacts labeled 3 in the middle region of FP are showed as two symmetrical broad peaks with minimum $d_e + d_i$ 2.1 Å (shorter than the sum of van der Waals radii), representing a 29.2% contribution to the entire HS area in this Cd complex. Finally, like in the structure CP1, the large deep-red spots labeled 2 in the d_{norm} map (Fig. 3) indicate also strong H···O/O···H interactions corresponding to the strongest N–H1C···OW hydrogen bond (Table 5), which also appear as two sharp symmetrical spikes at $d_e + d_i$ 1.90 Å in the FP with 5.5% contribution to the overall crystal packing.

The dominant XH/HX (X: Cl for Zn complex and I for Cd complex), OH/HO and HH interactions suggest that hydrogen bonding and van der Waals interactions play the main roles in the crystal packing of the two compounds.

3.3 Thermal analysis (DTA/TGA)

To investigate the thermal stability of compounds CP1 (Fig. 4) and CP2 (Fig. 5), thermal analysis (DTA/TGA) was carried out under an N_2 atmosphere with a heating rate of 10 °C/min in the temperature range from 25 to 600 °C. Overall, the TGA curves for these compounds indicate that the two H_2O molecules per formula unit are released between 25 and 130 °C. The experimental mass losses of 9.27% and 4.49% are in good agreement with the calculated values of 9.29% and 4.50% for CP1 and CP2, respectively. After dehydration, the anhydrous compound derivatives of CP1 and CP2 remain stable up to their melting points

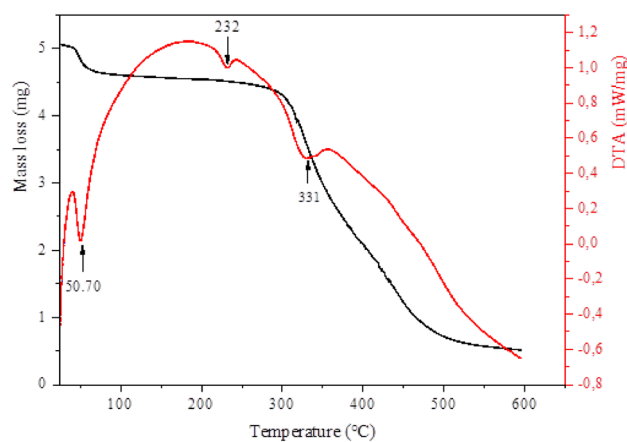


Fig. 4 Differential thermal DTA/thermogravimetric analysis TG of $(H_2CHBMA)ZnCl_4 \cdot 2H_2O$ (CP1)

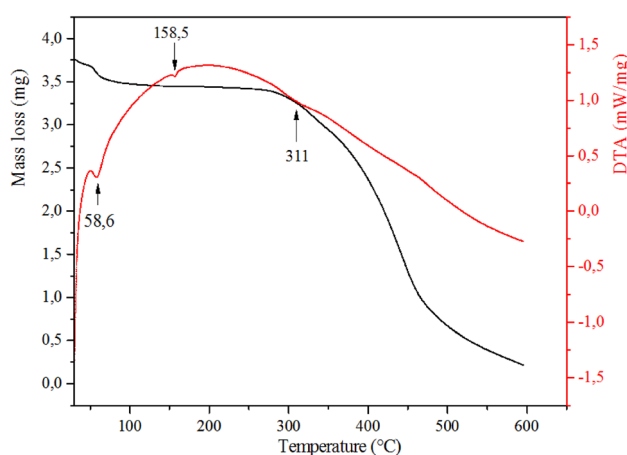


Fig. 5 Differential thermal DTA/thermogravimetric analysis TG of $(H_2CHBMA)CdI_4 \cdot 2H_2O$ (CP2)

at 225 °C and 153 °C, respectively. These melting points are confirmed by an additional thermal treatment in a separate furnace with run heating of 5 °C/min, from room temperature to 250 °C for CP1 and from room temperature to 200 °C for CP2. After that, the compounds undergo a considerable decomposition, suggesting the loss, among others, organic cations and the halogen atoms.

3.4 Spectroscopic study

3.4.1 ^{13}C NMR spectral analysis

High-resolution NMR spectroscopy is a powerful technique for the characterization of organic–inorganic hybrid materials.

The ^{13}C NMR solution spectrum of $(CBMH_2)ZnCl_4 \cdot 2H_2O$ (CP1) (Fig. 6) shows five signals at 24.14,

28.82, 32.98, 34.88 and 44.94 ppm due to the C₄, (C₃, C₅), C₁, (C₂, C₆) and (C₇, C₈), respectively. In fact, among the eight crystallographically independent carbons, we find the pairs (C₃, C₅), (C₂, C₆) and (C₇, C₈) that each one presents the same electronic environment. Therefore, they resonate at the same frequency and are characterized by the same chemical shift.

The ¹³C NMR solution spectrum of (CBMH₂)CdI₄·2H₂O (CP2) (Fig. 7) exhibits five signals corresponding to five carbon atoms crystallographically independent. From the spectrum, the signals centered at 24.45, 28.92, 32.79, 34.88 and 44.79 ppm are attributed to C₁, C₂, C₃, C₄ and C₅, respectively.

It is clear that the high values of chemical shifts are attributed to carbons (C₇, C₈) for CP1 C₁ for CP2, which are the closest to coordination place (N). This is explained by effect of the electronegative nitrogen atoms.

The low intensity signal observed experimentally at chemical shift 33.076 ppm, assigned to (C₂, C₆)

carbon atoms for CP1 and to C₂ carbon atoms for CP2, is due to the lack of attached protons.

3.4.2 Infrared spectra

To obtain further information upon the crystal structures of CP1 and CP2, we have undertaken vibrational analyses using infrared spectroscopy and Raman scattering. The IR absorption spectra of the two compounds CP1 (Fig. 8) and CP2 (Fig. 9) are similar, each showing clearly the bands corresponding only to vibrations of the 1,3-cyclohexanebis(methylammonium) cation, because the vibrational modes of ZnCl₄²⁻ or CdI₄²⁻ anions appear below 400 cm⁻¹ in IR spectrum. Therefore, the following IR analysis for the CP1 compound equally applies to the CP2.

Tentative attribution of the observed absorption bands is based on comparisons with the free organic molecule 1,3-cyclohexanebis(methylamine) and previously reported homologous compounds [35].

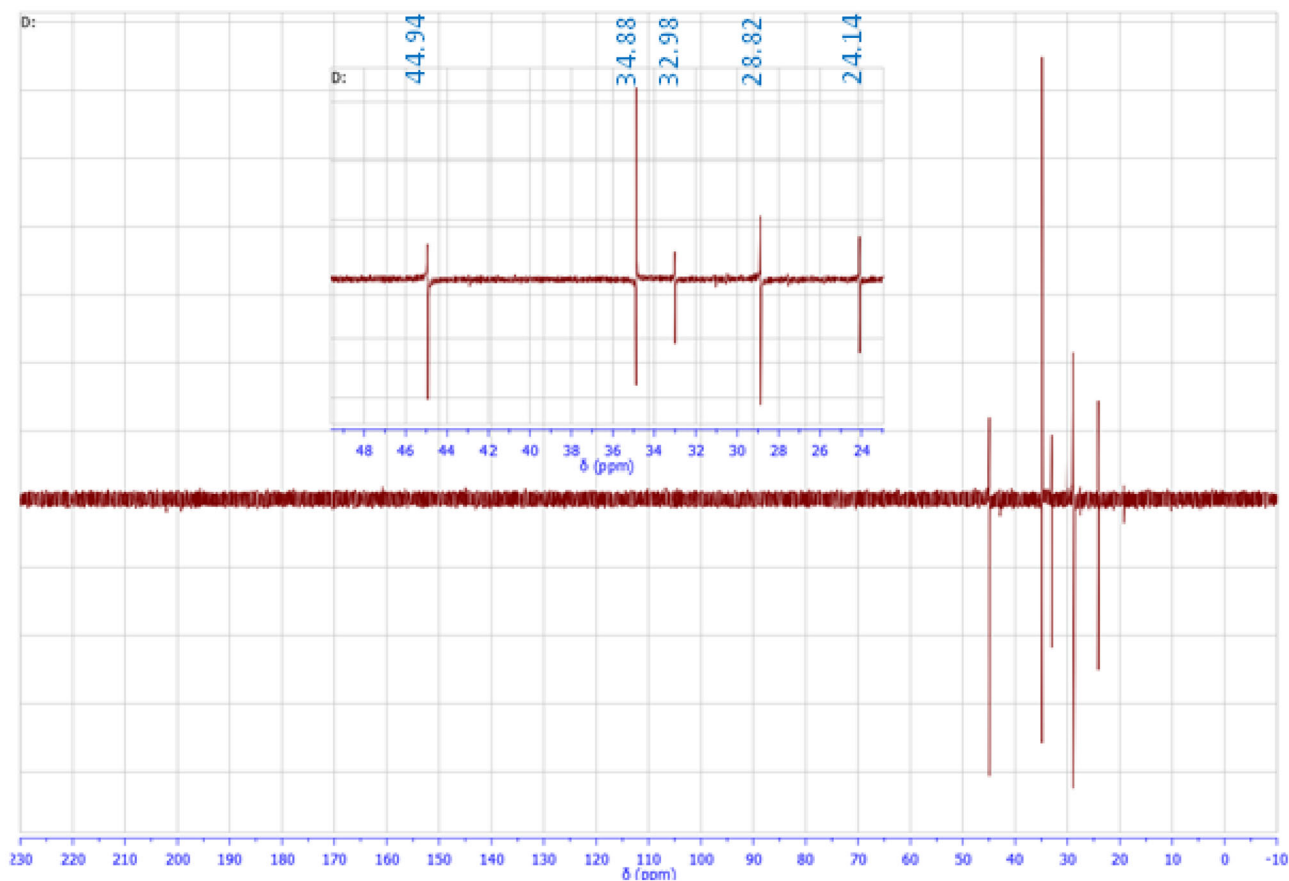


Fig. 6 ¹³C NMR spectrum of (H₂CHBMA)ZnCl₄·2H₂O (CP1)

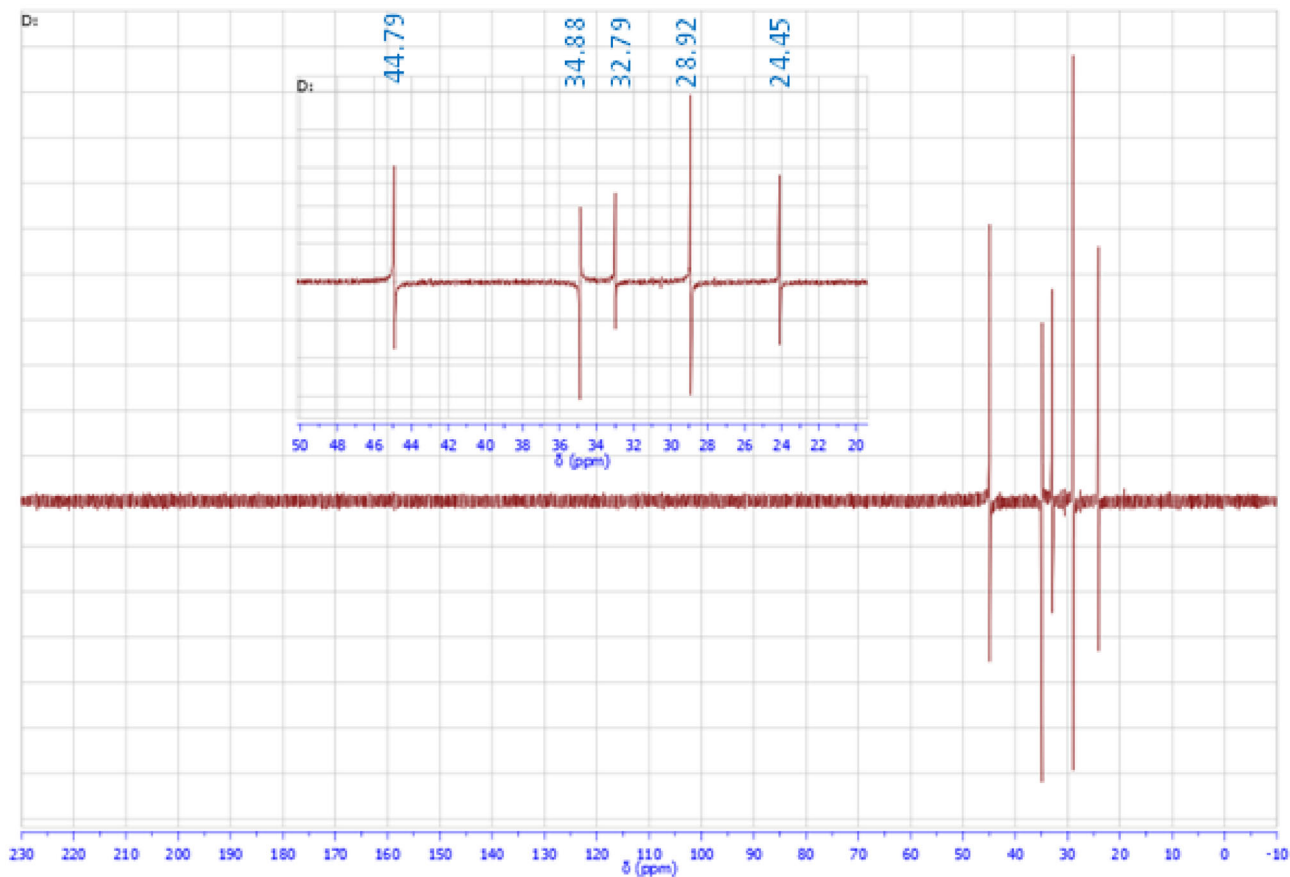


Fig. 7 ¹³C NMR spectrum of (H₂CHBMA)CdI₄·2H₂O (CP2)

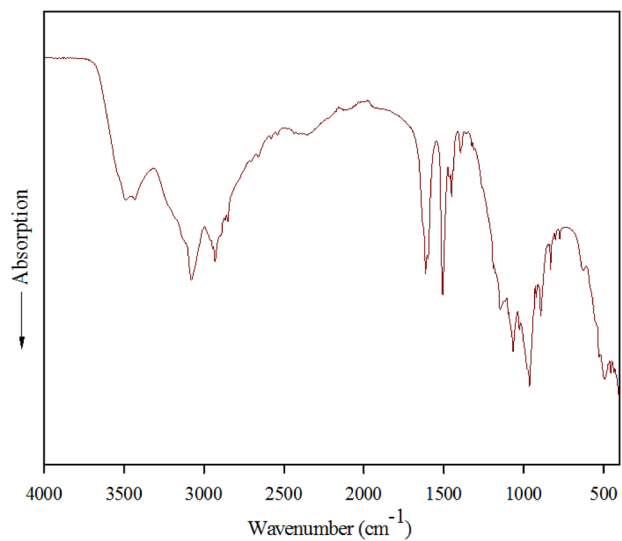


Fig. 8 Infrared spectrum of (H₂CHBMA)ZnCl₄·2H₂O (CP1)

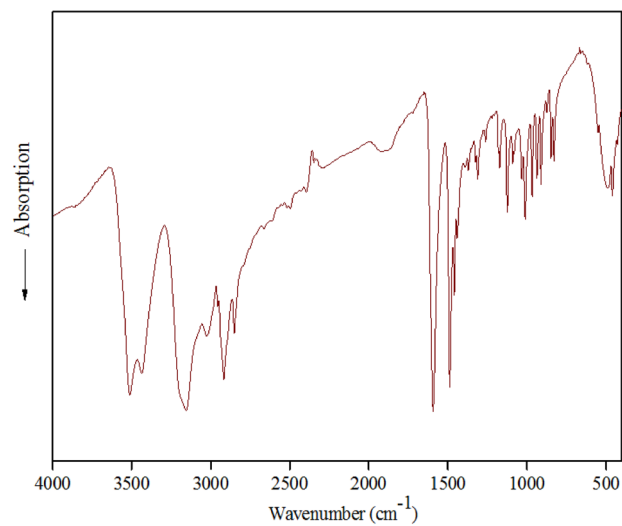


Fig. 9 Infrared spectrum of (H₂CHBMA)CdI₄·2H₂O (CP2)

The high-frequency region between 4000 and 2000 cm^{-1} in the spectrum is characterized by OH, NH and CH stretching modes, harmonics and combination bands.

- Water molecules vibration modes: Three bands are given for free water vibrational modes in the Tables of Molecular Vibrational Frequencies [36]. These frequencies are at 3756 cm^{-1} , 3657 cm^{-1} and 1595 cm^{-1} for the asymmetric stretching (ν_{as}), symmetric stretching (ν_{s}) and the bending (scissoring) (ν_{ip}) modes, respectively. The observed FTIR bands at 3487 cm^{-1} and 3422 cm^{-1} for CP1 and at 3514 cm^{-1} and 3438 cm^{-1} for CP2 are attributed, respectively, to asymmetric and symmetric stretching vibrations (O–H) of the crystallization water. As O–H of the crystallization H_2O is involved in hydrogen bonds $\text{OH}\cdots\text{N}$ and $\text{OH}\cdots\text{Cl(I)}$, the wave numbers of these modes are shifted towards lower values. The (H_2O) deformation mode is determined at 1608 cm^{-1} for CP1 and at 1595 cm^{-1} for CP2 in the FTIR spectra.
- Vibration of NH_3^+ groups: The amino groups of 1,3-cyclohexanebis(methylamine) are protonated. The NH_3^+ group may vibrate mainly in three different modes, namely, asymmetric stretching (ν_{as}), symmetric stretching (ν_{s}) and the in plane bending mode (ν_{ip}). The observed FTIR bands at 3133 cm^{-1} and 3077 cm^{-1} for CP1 (Fig. 8) and those observed at 3153 cm^{-1} and 3028 cm^{-1} for CP2 (Fig. 9) are assigned to asymmetric and symmetric NH_3^+ stretching, respectively. These frequencies of the stretching modes of NH_3^+ groups in the title compounds are lower compared to $-\text{NH}_2$ frequencies ($\nu_{\text{as}} = 3371 \text{ cm}^{-1}$, $\nu_{\text{s}} = 3292 \text{ cm}^{-1}$) in 1,3-cyclohexanebis(methylamine). The most reasonable reason for this difference is the modification of NH_2 chemical environment as a result of $\text{N-H}\cdots\text{Cl(I)}$ and $\text{N-H}\cdots\text{O}$ hydrogen-bond formation. The NH_3^+ in plane bending vibration is found to be at 1502 cm^{-1} for CP1 and 1489 cm^{-1} for CP2.
- Vibration of CH_2 group: The CH_2 group may vibrate in different fashions, namely, asymmetric stretching, symmetric stretching and the in plane bending mode: In this instance, the CH_2 asymmetric and symmetric stretch vibrations appear, respectively, at 2922 cm^{-1} and 2879 cm^{-1} for CP1 and at 2921 cm^{-1} and 2854 cm^{-1} for CP2. The band located at 1450 cm^{-1} (Fig. 8) and that located

at 1441 cm^{-1} (Fig. 8) are due to the ($-\text{CH}_2-$) scissor mode, while the bands observed at 1439 cm^{-1} and 1390 cm^{-1} and those observed at 1434 cm^{-1} and 1392 cm^{-1} (Fig. 9) are ascribed to asymmetric and symmetric deformation modes of the ($-\text{CH}_2-$), respectively.

- Harmonics and combination bands: The bands situated in the 2550–2000 cm^{-1} region are ascribed to the harmonics and combination bands.
- Vibrations of C–N and C–C groups: The medium intensity absorption band observed at 1137 cm^{-1} for CP1 and that observed at 1125 cm^{-1} for CP2 correspond to the stretching vibration mode of C–N, while the stretching vibration mode of C–C bond is not detected on the IR spectra because of the low intensity of the corresponding absorption band.

3.4.3 Raman spectra

The presence of a heavy metal atom in a tetrahedral coordination, such as ZnCl_4^{2-} or CdI_4^{2-} , gives rise to low-frequency vibration modes which appear below 350 cm^{-1} in Raman spectrum.

Typically, the ideally tetrahedral MX_4 (ZnCl_4^{2-} , CdI_4^{2-}) generates nine basal vibrations, as follows: $1(\text{A}_1)$ and $3(\text{F}_2)$ correspond to M–X (Zn–Cl, Cd–I) stretching vibrations; $2(\text{E})$ and $4(\text{F}_2)$ correspond to X–M–X (Cl–Zn–Cl, I–Cd–I) deformation vibrations. In the crystal, the ideally tetrahedral MX_4 (ZnCl_4^{2-} , CdI_4^{2-}) is deformed and as a result there is a splitting on the vibrational modes of E and F2 symmetries.

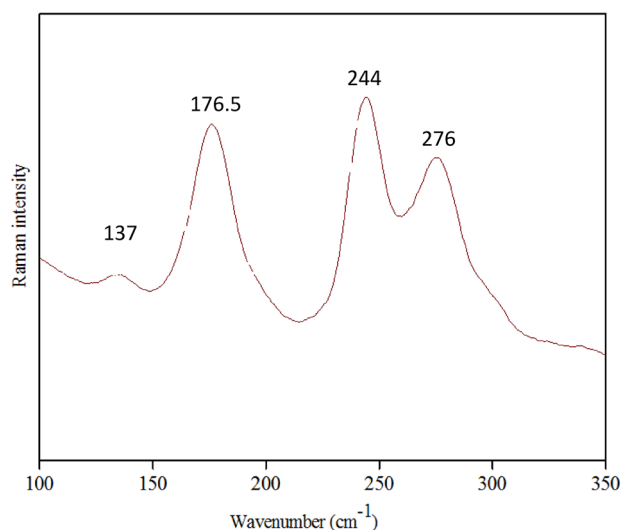


Fig. 10 Raman spectrum of $(\text{H}_2\text{CHBMA})\text{ZnCl}_4 \cdot 2\text{H}_2\text{O}$ (CP1) in the region 100–350 cm^{-1}

Figure 10 shows the Raman spectrum of $(\text{CBMH}_2)\text{ZnCl}_4 \cdot 2\text{H}_2\text{O}$. According to previous studies and by comparison with the Raman spectrum of analogous compounds containing ZnCl_4^{2-} , we may propose a tentative attribution of the observed bands [14, 37]. The bands observed at 244 and 276 cm^{-1} can be allocated to the symmetric and asymmetric Zn–Cl stretching modes of ZnCl_4^{2-} . The bands at 137 cm^{-1} and 176.5 cm^{-1} can be assigned to the symmetric and asymmetric bending mode of Cl–Zn–Cl bonds.

Figure 11 shows the Raman spectrum of $(\text{CBMH}_2)\text{CdI}_4 \cdot 2\text{H}_2\text{O}$. The bands at 115.4 and 125.3 cm^{-1} can be attributed to the symmetric and asymmetric Cd–I stretching modes that are in good agreement with other tetrahedral compounds with CdI_4^{2-} [30, 38]. The band at 54 cm^{-1} can be assigned to the I–Cd–I deformation mode.

As is clear from the above discussion, these FT–IR and Raman spectroscopic results were coherent with the single-crystal X-ray results.

4 Conclusion

In summary, $(\text{H}_2\text{CHBMA})\text{ZnCl}_4 \cdot 2\text{H}_2\text{O}$, (CP1), and $(\text{H}_2\text{CHBMA})\text{CdI}_4 \cdot 2\text{H}_2\text{O}$, (CP2), have been synthesized by conventional methods under the acidic conditions supplied by hydrochloric acid and sulfuric acid, respectively. X-ray diffraction analysis reveals that the two compounds CP1 and CP2 crystallize in the same monoclinic crystal system with space

groups ($P2_1/c$) and ($P2_1/m$), respectively. The crystals packing of the two compounds are stabilized by non-covalent interactions which are in close agreement with the Hirshfeld surface analysis. Albeit the template H_2CHBMA adopts a cis configuration in both compounds, CP1 presents 2D H-bonded architecture, while CP2 shows a diamond 3D... H-bonded framework. By comparing the structures of CP1 and CP2, we can discover the role of the orientations of two terminal ammonium groups (upward for CP1 and downward for CP2) of the organic cation in controlling the different supramolecular architectures. Interestingly, while the templates sit in the cis configuration in both compounds CP1 and CP2, they are in the trans configuration in other compounds. This result has the potential for separation and recognition of CHBMA isomers.

The thermal analyses of these compounds were examined by TGA/DTA and the results indicate that all the H_2O molecules are released between 25 and $120\text{ }^\circ\text{C}$ and that the anhydrous compound derivative of CP1 is more stable than that of CP2. The FT–IR, Raman and ^{13}C NMR spectroscopic results are in agreement with the single-crystal X-ray results.

The synthesized compounds were evaluated for acetalization reaction of aldehydes and demonstrated high catalytic activity which will be published later in a new paper.

5 Supplementary material

CCDC 1825834 and 1563308 contain the supplementary crystallographic data for this paper. These data can be obtained free of charge via http://www.ccdc.cam.ac.uk/data_request/cif, by e-mailing data_request@ccdc.cam.ac.uk or by contacting The Cambridge Crystallographic Data Centre, 12 Union Road, Cambridge CB2 1EZ, UK. Fax: + 44 1223 336033.

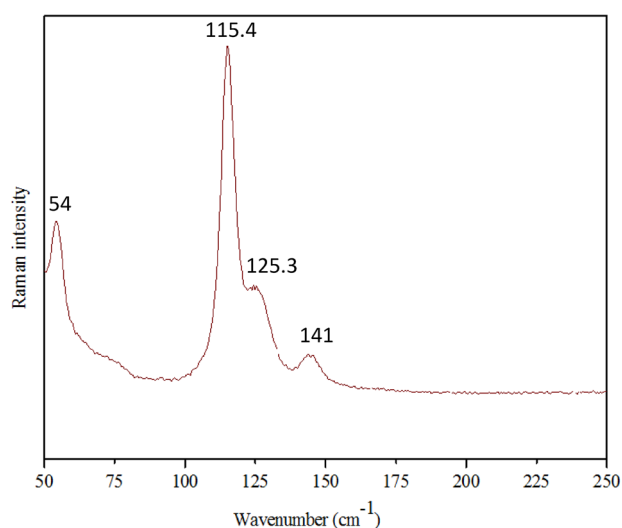


Fig. 11 Raman spectrum of $(\text{H}_2\text{CHBMA})\text{CdI}_4 \cdot 2\text{H}_2\text{O}$ (CP2) in the region $50\text{--}250\text{ cm}^{-1}$

Open Access This article is licensed under a Creative Commons Attribution 4.0 International License, which permits use, sharing, adaptation, distribution and reproduction in any medium or format, as long as you give appropriate credit to the original author(s) and the source, provide a link to the Creative Commons licence, and indicate if changes were made. The images or other third party material in this article are included in the article's Creative Commons licence, unless indicated otherwise in a credit line to the material. If material is not included in the article's Creative Commons licence and your intended use is not permitted by statutory regulation or exceeds the permitted use, you will need to obtain permission directly from the copyright holder. To view a copy of this licence, visit <http://creativecommons.org/licenses/by/4.0/>.

References

- K. Rurack, R. Martinez-Manez, *The Supramolecular Chemistry of Organic-Inorganic Hybrid Materials* (Wiley, Hoboken, 2010).
- M. Nanko, *Adv. Technol. Mater. Mater. Process. J.* **11**(1), 1–8 (2009)
- F.A. Afkhami, A.A. Khandar, G. Mahmoudi, W. Maniukiewicz, A.V. Gurbanov, F.I. Zubkov, O. Şahin, O.Z. Yesilel, A. Frontera, *CrystEngComm* **19**, 1389–1399 (2017)
- S.C. Van Wyk, M.O. Onani, E. Nordlander, *Chem. Pap.* **70**(8), 1003–1023 (2016)
- N. Hfidhi, I. Bkhairia, D. Atoui, J. Boonmak, M. Nasri, R. Ben Salem, S. Youngme, H. Naili, *Appl. Organomet. Chem.* **33**(4), 4793 (2019)
- J.Y. Ryu, J.H. Han, J.Y. Lee, S.J. Hong, S.H. Choi, C. Kim, S.-J. Kim, Y. Kim, *Inorg. Chim. Acta* **358**, 3659–3670 (2005)
- Y. Liu, L. Liu, X. Zhang, G. Liangand, X. Gong, *Acta Cryst.* **74**, 13–20 (2018)
- H. Tapiero, K.D. Tew, *Biomed. Pharmacother.* **57**, 399–411 (2003)
- N. Farrell, *Coord. Chem. Rev.* **232**, 1–4 (2002)
- F.A.A. Paz, J. Klinowski, S.M.F. Vilela, J.P.C. Tome, J.A.S. Cavaleiroc, J. Rochaa, *Chem. Soc. Rev.* **41**, 1088–1110 (2012)
- D.B. Mitzi, *Chem. Mater.* **8**, 791–800 (1996)
- M.L. Mrada, I. Feddaouia, M.S.M. Abdelbakyc, S. García-Grandac, C. Ben Nasr, *Inorg. Chim. Acta* **476**, 38–45 (2018)
- N.M. Rhoumaa, A. Rayes, F. Mezzadric, D. Delmonted, R. Cabassid, G. Calestanic, M. Loukil, J. Solid State Chem. **256**, 60–66 (2017)
- M. Ben Bechir, K. Karoui, A. Bulou, M. Tabellout, K. Guidara, A. Ben Rhaïem, *J. Appl. Phys.* **116**, 214104 (2014)
- K. Karoui, A. Ben Rhaïem, F. Jomni, J.L. Moneger, A. Bulou, K. Guidara, *J. Mol. Struct.* **1048**, 287–294 (2013)
- K. Karoui, A. Ben Rhaïem, K. Guidara, *Phys. B* **407**, 489–493 (2012)
- A.R. Lim, P. Bong, S. Jeong, *Solid State Commun.* **143**, 432–436 (2007)
- S. Sato, D. Nakamura, *Bull. Chem. Soc. Jpn.* **60**, 463–475 (1987)
- A.M. Ben Salah, L.B. Fendri, T. Bataille, R.P. Herrera, H. Naili, *Chem. Cent. J.* **12**(1), 1–12 (2018)
- H. Naili, F. Hajlaoui, T. Mhiri, T.C.O.M. Leod, M.N. Kopylovich, K.T. Mahmudov, A.J.L. Pombeiro, *Dalton Trans.* **42**, 399–406 (2013)
- M.J. Turner, J.J. McKinnon, S.K. Wolff, D.J. Grimwood, P.R. Spackman, D. Jayatilaka, M.A. Spackman, *Crystal Explorer 17.5* (University of Western Australia, Perth, 2017).
- N. Leesakul, W. Runrueng, S. Saithong, C. Pakawatchai, *Acta Cryst.* **E68**, m837 (2012)
- N.M. Rhouma, A. Rayes, F. Mezzadri, G. Calestani, M. Loukil, *Acta Cryst. E* **72**, 1050–1053 (2016)
- J. Granifo, S. Suarez, F. Boubeta, R. Baggio, *Acta Cryst. C* **73**, 1121–1130 (2017)
- R. Kefi, E. Jeanneau, F. Lefebvre, C. BenNasr, *Acta Cryst. C* **67**, m126–m129 (2011)
- L. Yang, D.R. Powell, R.P. Houser, *Dalton Trans.* (2007). <https://doi.org/10.1039/B617136B>
- D. Altermatt, I.D. Brown, *Acta Cryst. A* **43**, 125–130 (1987)
- M.C. Etter, *Acc. Chem. Res.* **23**, 120–126 (1990)
- Y. Yang, Y. Zhao, J. Yu, S. Wu, R. Wang, *Inorg. Chem.* **47**(3), 769–771 (2008)
- A. Kessentini, M. Belhouchet, J.J. Suñol, Y. Abid, T. Mhiri, J. Mol. Struct. **1039**, 207–213 (2013)
- R.D. Bailey, W.T. Pennington, *Acta Cryst. C* **51**, 226–229 (1995)
- H. Ishihara, K. Horiuchi, T.M. Gesing, S.-Q. Dou, J.-C. Buhl, P. Erk, Z. Naturforschung **57**, 503–508 (2002)
- H. Chebbi, S. Mezrigui, M. Ben Jomaa, M.F. Zid, *Acta Cryst. E* **74**, 949–954 (2018)
- P. Venkatesan, S. Thamocharan, A. Ilangovan, H. Liang, T. Sundius, *Spectrochim. Acta A* **153**, 625–636 (2016)
- A. Rayes, R.P. Herrera, M. Moncer, I. Ara, G. Calestani, B. Ayed, F. Mezzadri, *J. Mol. Struct.* **1202**, 127216 (2020). <https://doi.org/10.1016/j.molstruc.2019.127216>

36. T. Shimanouchi, *Tables of Molecular Vibrational Frequencies Consolidated*, vol. I (National Standard Reference Data System, Tokyo, 1972).
37. M.E.C. Villalba, G. Echeverría, P.J. Aymonino, E.L. Varetti, *J. Chem. Crystallogr.* **41**, 508–513 (2011)
38. M. Ghanbari, S. Gholamrezaei, M. Salavati-Niasari, *J. Alloys Compd.* **667**, 115–122 (2016)

Publisher's Note Springer Nature remains neutral with regard to jurisdictional claims in published maps and institutional affiliations.